

# High-Power Mid-IR (4–5 $\mu\text{m}$ ) Femtosecond Laser System with a Broadband Amplifier Based on $\text{Fe}^{2+}:\text{ZnSe}$

B. G. Bravy<sup>c</sup>, V. M. Gordienko<sup>a,b</sup>, V. I. Kozlovsky<sup>d,e</sup>, Yu. V. Korostelin<sup>d</sup>, F. V. Potemkin<sup>a,b</sup>,  
Yu. P. Podmar'kov<sup>d,f</sup>, A. A. Podshivalov<sup>b</sup>, V. T. Platonenko<sup>a,b</sup>, V. V. Firsov<sup>b,g</sup>, and M. P. Frolov<sup>d,f</sup>

<sup>a</sup>Faculty of Physics, Moscow State University, Moscow, 119991 Russia

<sup>b</sup>International Laser Center, Moscow State University, Moscow, 119991 Russia

<sup>c</sup>Institute of Problems of Chemical Physics, Russian Academy of Sciences, Chernogolovka, Moscow oblast, 142432 Russia

<sup>d</sup>Lebedev Physical Institute, Russian Academy of Sciences, Moscow, 119991 Russia

<sup>e</sup>National Research Nuclear University, Moscow Engineering Physics Institute (MEPhI), Moscow, 115409 Russia

<sup>f</sup>Moscow Institute of Physics and Technology (State University), Dolgoprudny, Moscow oblast, 141700 Russia

<sup>g</sup>Skobel'tsyn Institute of Nuclear Physics, Moscow State University, Moscow, 119991 Russia

e-mail: [potemkin@physics.msu.ru](mailto:potemkin@physics.msu.ru)

**Abstract**—Concept of a solid-state femtosecond laser system with a multigigawatt power level in the 4–5  $\mu\text{m}$  range has been proposed. The system contains an ultrashort pulse seeder, a two-stage chirped pulse amplifier based on a broadband  $\text{Fe}^{2+}:\text{ZnSe}$  active element with optical pumping by a YSGG:Cr:Er laser, and an output stage that provides additional nonlinear optical compression of an amplified pulse to approximately 30 fs in a dielectric  $\text{CaF}_2$  medium with anomalous group velocity dispersion in this spectral range.

DOI: 10.3103/S1062873816040055

## INTRODUCTION

In this work, we review the design concept and parameters of individual parts of a femtosecond laser system with the subterawatt power level of the middle IR range (4–5  $\mu\text{m}$ ), operating on the principle of amplifying an ultrashort seed light pulse in an optically pumped amplifier driven by a zinc selenide crystal doped with iron ions ( $\text{Fe}^{2+}:\text{ZnSe}$ ). The execution of this design relies, among other things, on the reported results concerning the efficient lasing of a  $\text{Fe}^{2+}:\text{ZnSe}$  laser at room temperature with pumping by solid-state and HF lasers [1–3]. The results from calculations for the self-compression of amplified femtosecond radiation are also detailed below. The calculations were performed using the approach proposed in [4] and were based on spectrum broadening due to the Kerr nonlinearity in  $\text{CaF}_2$  and the subsequent compression of a femtosecond pulse in the regime of anomalous group velocity dispersion.

## A FEMTOSECOND LASER SYSTEM OF THE 4–5 $\mu\text{m}$ RANGE

The spectroscopic features of a  $\text{Fe}^{2+}:\text{ZnSe}$  crystal [5] allow us to amplify ultrashort IR laser pulses with durations of approximately 50 fs. Since the lifetime of the upper working level of a  $\text{Fe}^{2+}:\text{ZnSe}$  crystal at room temperature is 370 ns [1], both YSGG:Cr:Er and

YAG:Er lasers with Q-switching [5, 6], or a non-chain electrodischarge HF laser [3], can be used as the high-power optical pumping source. The wavelengths of these lasers fall within the  $\text{Fe}^{2+}:\text{ZnSe}$  absorption band, and the lasing pulse width does not exceed 150 ns.

According to the proposed design concept, a high-power femtosecond laser system based on  $\text{Fe}^{2+}:\text{ZnSe}$  should include a multipass amplifying circuit for a seed chirped pulse and a unit for the subsequent compression of the amplified laser pulse. Let us characterize each unit of a high-power femtosecond laser system of the middle IR range separately.

### *Generator of Seed Radiation Pulses in the 4–5 $\mu\text{m}$ Range*

A subpicosecond pulse produced by a two-stage optical parametric amplifier (OPA), the design of which was developed and executed earlier in the 10-micrometer range [7], serves as the injection pulse in the middle IR range for the amplifying stage. The first stage of the parametric generator of the middle IR range (with a BBO crystal, type II interaction) is pumped by second-harmonic radiation from a Cr:forsterite laser (620 nm, 100 fs, and 200  $\mu\text{J}$ ) and is mixed with supercontinuum radiation produced by focusing a small fraction of the primary emission of the Cr:forsterite laser onto a sapphire crystal.

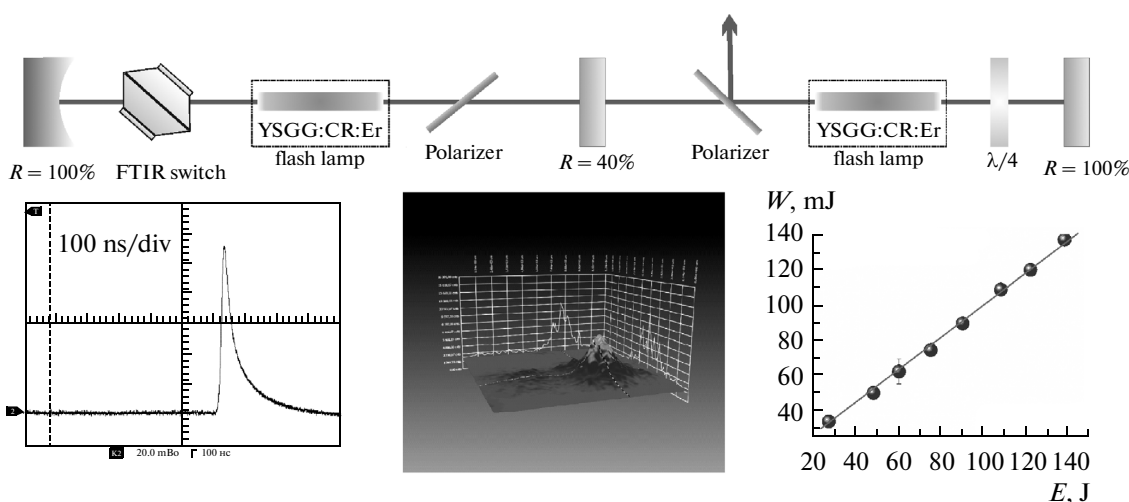


**Fig. 1.** First row: diagram of the YSGG:Cr:Er laser operated in the Q-switching mode with a two-pass amplifier and polarization isolation. Second row, left to right: measurements of the pulse duration using an avalanche photodiode; pumping beam mode; and dependence of the pulse energy at the output of the generator–amplifier system on the pumping energy (the energy of the amplified pulse at the amplifier input was 35 mJ; the pulse duration was approximately 60 ns).

At the second stage of the IR OPA based on a silver thiogallate crystal, frequency downconversion occurs during the nonlinear optical mixing of idler radiation from the first OPA stage (with a wavelength of 1.5–1.8  $\mu\text{m}$ ) with the pumping pulse (the remainder of the initial pulse of the primary emission from a chromium–forsterite laser with a wavelength of 1240 nm and an energy of 300  $\mu\text{J}$ ). As a result of parametric amplification, a seed radiation pulse in the middle IR range with a wavelength of 4–5  $\mu\text{m}$ , a width of 200 fs, and an energy of 0.1–0.2  $\mu\text{J}$  is generated at the output of the second OPA stage.

This 200-femtosecond pulse with a wavelength of 4–5  $\mu\text{m}$  is then temporally stretched out by a factor of around 2000 using a grating-based (150 lines/mm) stretcher to reduce the peak power proportionally. This helps avoid the effects of small-scale radiation self-focusing in a multipass two-stage amplifier. The duration of the seed pulse was estimated using a correlation technique based on a sum-frequency generation scheme.

#### *Multipass Amplifier Based on $\text{Fe}^{2+}:\text{ZnSe}$*

The multipass amplifier based on  $\text{Fe}^{2+}:\text{ZnSe}$  is pumped by a YSGG:Cr:Er laser (2.79  $\mu\text{m}$ ) with Q-switching. As was already noted, the radiation wavelength of this laser is close to the absorption band maximum of active iron ions in the ZnSe matrix [4].

#### *YSGG:Cr:Er Optical Pumping Laser*

Using Russian electronic components, we designed and constructed a solid-state YSGG:Cr:Er laser with Q-switching based on frustrated total internal reflection and a two-pass amplifier with polariza-

tion isolation with an output power of approximately 140 mJ at a generated pulse duration of 60 ns [8]. The schematic diagram of the setup is shown in Fig. 1.

The linearly polarized YSGG:Cr:Er laser radiation passes through a thin-film polarizer and is injected into the two-pass amplifier based on a YSGG:Cr:Er crystal with a length of 90 mm and a diameter of 4 mm. After passing twice through a quarter-wave plate made from  $\text{MgF}_2$ , the polarization plane is rotated, and the amplified radiation is then reflected from the thin-film polarizer. Assisted by two mirrors, it is used to pump the laser or the multipass amplifier based on  $\text{Fe}^{2+}:\text{ZnSe}$ . The operation of the supply units of the laser, the amplifier, and the modulator control unit is synchronized by synchronization pulses produced by the laser supply unit. A gain factor of 4.4 was obtained at an amplifier pumping energy of about 120 J.

The dependence of the amplifier output energy on the pumping energy was then determined (see Fig. 1). The measured time jitter of the solid-state YSGG:Cr:Er laser with Q-switching based on the frustrated total internal reflection was 120 ns. Since this value lies within the margin of instability for triggering the electronic switch in lasers pumping the femtosecond OPA, such a setup can be used to synchronize two lasers. The relatively long lifetime of the upper excitation level of the amplifier allows us to conduct experiments with time jitters of 120 ns even at room temperature by slightly varying the inversion and gain factor.

#### *Multipass Amplifier Based on $\text{Fe}^{2+}:\text{ZnSe}$*

So far as we know, the amplification of ultrashort IR laser pulses by a  $\text{Fe}^{2+}:\text{ZnSe}$  amplifier with optical pumping has yet to be studied. The available literature

Values of the parameters used to calculate the energy of a pulse at the amplifier output

	$E_{in}$ , $\mu\text{J}$	$D_{in}$ , mm	$g_0L$	$R$ , %
First stage	1	2	0.8	2
Second stage	50	4	0.8	2

data provide an opportunity to determine tentatively the conditions under which the needed output energy can be obtained.

The seed pulse energy in our setup is on the order of several microjoules. This allows us to use the multipass amplification scheme. This approach strongly differs from when the master generator produces low-energy (about 1 nJ, which is typical of femtosecond laser systems based on, e.g., Cr:forsterite [9] or Cr:ZnSe [10]) pulses, and the low level of seed radiation requires the use of a regenerative amplification circuit to reach, e.g., the submillijoule energy level.

The total pumping energy used in the setup is 100 mJ at a pulse duration of approximately 60 ns. The pumping is split into two channels (20 and 80 mJ) and is fed into two stages of multipass amplification at a narrow angle, thus eliminating the need for a dichroic mirror. In order to obtain the optimum gain factor at both stages, a pumping energy density in the active crystal of no less  $0.5 \text{ J cm}^{-2}$  must be ensured. This is because the pumping beam has a size of 2 mm in the first stage and expands to 4 mm prior to entering the second stage.

The pumping pulse is synchronized with the passage of the amplified pulse by tuning the corresponding delays at two electrooptical Q-switches (of the YSGG:Cr:Er laser and the Nd:YAG pumping laser in the femtosecond laser system amplifier based on chromium–forsterite) with a specialized two-channel electronic synchronization unit. The instability of the times of arrival of light pulses at the level of  $\pm 20$  ns does not alter the gain factor appreciably. In fact, it provides an opportunity to use several independent solid-state pumping lasers synchronized by an electric pulse and thus raise the overall pumping power.

Note that slight cooling (to  $10^\circ\text{C}$ , which is easily achieved using thermoelectric Peltier elements) of the  $\text{Fe}^{2+}:\text{ZnSe}$  active elements extends the lifetime of the active level to 1  $\mu\text{s}$ . This relaxes the requirements for the mutual synchronization of the amplified pulse and the pumping pulse. To reach the working level, the overall gain factor of the two-stage multipass amplifier must be as high as  $10^3$ – $10^4$ . Amplification in the last pass proceeds in the saturation regime.

The multipass amplifier design can be optimized by maximizing its efficiency. This is reduced to first finding the optimum cross section of pumping beams and the amplified signal in the active element, and then

determining the optimum number of passes of the amplified radiation through the active medium.

We calculated the process of two-stage multipass amplification. It was assumed that the pumping and injection beams in the crystal were perfectly matched. It was also considered that the amplified laser radiation propagates within the amplifier without losses (this can be achieved in practice if the residual air pressure is reduced in the amplifier). The Frantz–Nodvik formula [11], which considers the amplifying medium within a two-level approach, was used to calculate the pulse amplification in the saturation regime.

The following quantities were used as the input parameters in our calculations: input energy  $E_{in}$  of the injected pulse, waist diameter  $D$  of the injected pulse in the crystal, nonresonance losses  $R$  in the amplifier per one pass (the losses in the amplifier per one pass minus the losses associated with absorption in the crystal), crystal length  $L$ , and effective gain factor  $g_0$  for a weak signal taking into account probable losses for spontaneous luminescence in the transverse direction and absorption of the generated radiation in the active medium.

Active medium length  $L = 0.8$  cm and saturation energy density  $\varphi_{sat} = 30 \text{ mJ cm}^{-2}$  were set. The value of  $\varphi_{sat}$  was estimated using a formula valid for a four-level system:  $E_{sat} \sim h\nu/\sigma$ , where  $h\nu \sim 4.6 \times 10^{-20} \text{ J}$  is the energy of a quantum and  $\sigma \sim 1.5 \times 10^{-18} \text{ cm}^2$  is the cross section of the stimulated transition [5]. Optimization of the number of passes at a constant output energy in the middle IR range of 4 mJ showed that the optimum amplification scheme is a two-stage one with twofold expansion of the injection beam at the output of the first stage (see table).

Our results (see Fig. 2) show that the optimum (in terms of minimizing the number of passes through the  $\text{Fe}^{2+}:\text{ZnSe}$  active element) amplification scheme is an injection beam with a diameter of 2 mm, amplified in five passes in the first stage to an energy of  $\sim 100 \mu\text{J}$ , expanded to 4 mm, again amplified in five passes to an energy of 4 mJ, and then sent to the amplifier output. The indicated values are sufficient to obtain an output energy of 2 mJ after compression. It is important that such energy is attained at the amplifier output after ten passes. These figures are easily achieved if the amplifier is designed with two stages in the X configuration.

Note that although the ZnSe matrix has the relatively high nonlinear coefficient  $n_2 \sim 10^{-14} \text{ cm}^2 \text{ W}^{-1}$  [12], its influence on the last pass in the amplifier should not affect the beam quality in terms of small-

scale self-focusing:  $B = \frac{2n_0 E}{\lambda \rho_0^2 \tau} n_2 L \cong 0.01 \ll 2$ , where

wavelength  $\lambda = 4.5 \mu\text{m}$ , refraction coefficient of the ZnSe matrix  $n_0 = 2.43$ , crystal length  $L = 0.8$  cm, energy  $E = 4$  mJ, pulse duration  $\tau = 300$  ps, and injection spot radius  $\rho_0 = 0.4$  cm.

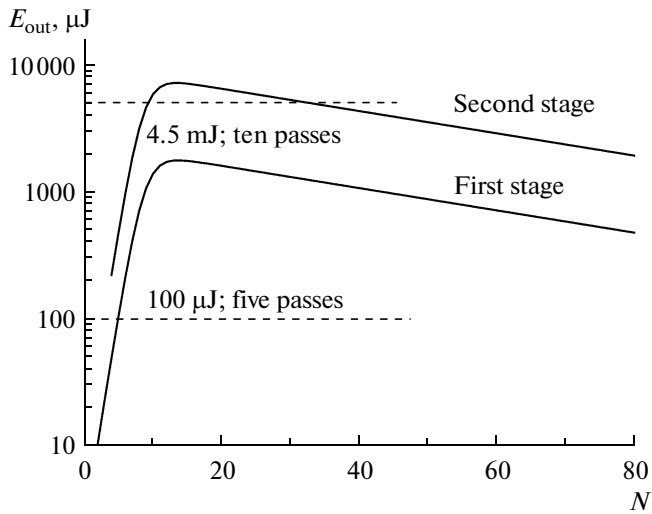


**Fig. 2.** Calculated dependence of the output energy of an amplified pulse on number of passes  $N$  through the active element in the two-stage amplifier.

#### *Experiments in the Free-Running Mode of the $\text{Fe}^{2+}:\text{ZnSe}$ Laser*

We conducted preliminary experiments focused on investigating the parameters of free-running lasing in order to determine the optimum pumping energy density and estimate the possible influence of thermal effects on the amplification regime. A zinc selenide crystal (doped with ferrous iron with a concentration of  $2.5 \times 10^{18} \text{ cm}^{-3}$ ) was used. The optical pumping propagated at an angle of  $5^\circ$  to the optical axis of a cavity with a length of 200 mm and the optimum output mirror with a reflection coefficient of 40%.

Figure 3 shows the dependence of the output energy on the absorbed optical pumping energy at a maximum pumping energy density of  $0.6 \text{ J cm}^{-2}$ . It turns out that the differential efficiency of conversion with respect to the incident (absorbed) energy was close to 15% (30%). These values agree with the results obtained in [5, 6]. Note that the available literature data suggest that the optimum pumping energy density is approximately inversely proportional to the pumping pulse duration, and the lasing efficiency is limited by the radiation stability of  $\text{Fe}^{2+}:\text{ZnSe}$  ( $1 \text{ J cm}^{-2}$  in the present case).

Our experimental results on the output laser energy in the free-running mode (3–4 mJ) thus provided the upper bound for the probable energy of a pulse amplified in the multipass regime. The lasing development time was also measured. The obtained value (10–20 ns) allows us to measure experimentally the amplification of a weak signal with no loss in amplification.

The amplified pulse should then be fed through a nonlinear optical compressor (an element made of an

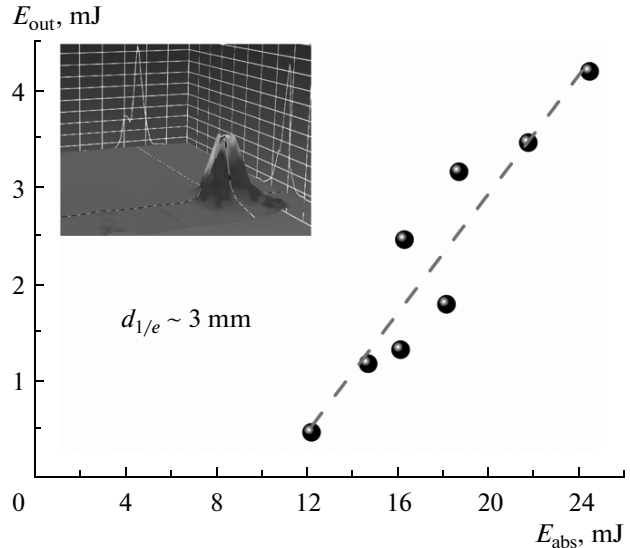


**Fig. 3.** Dependence of the output pulse energy on the optical pumping energy absorbed in the  $\text{Fe}^{2+}:\text{ZnSe}$  crystal. The inset shows the mode of the lasing beam, captured with a Pyrocam III camera based on a pyroelectric array.

IR material with anomalous group velocity dispersion in the range of 4–5  $\mu\text{m}$ ).

#### SELF-COMPRESSION OF FEMTOSECOND PULSES IN A TRANSPARENT DIELECTRIC

Our calculation model was based on the approaches used for high-power 10-micrometer laser pulses in [4]. It was assumed that the pulse duration should be reduced by a factor of no less than 3 due to self-compression, while the planned peak power of the laser system should be tripled and reach a minimum of 10 GW in the 4–5  $\mu\text{m}$  interval, which is beyond the range of modern commercial systems based on the parametric frequency conversion of laser radiation. Since  $\text{CaF}_2$  had the maximum magnitude of dispersion of group velocity (calculated using the dispersion relations from [13]), it was used as the nonlinear medium for the self-compression of femtosecond pulses of the middle IR range and helped minimize the length of this medium. Nonlinear refraction coefficient  $n_2 = 1.9 \times 10^{-16} \text{ cm}^2 \text{ W}^{-1}$  was taken from [14]. The breakdown threshold of  $\text{CaF}_2$  exceeds  $5 \times 10^{12} \text{ W cm}^{-2}$  [15]. Energy gap width  $E_g = 12.3 \text{ eV}$  [16].

The evolution of an ultrashort pulse in the medium was calculated using the nonlinear Schrödinger equation [17] for a light pulse with a wide spectrum and a duration of up to a single period. The volume ionization rate in the kinetic equation characterizing the dynamics of free electrons was calculated using the formulas from [18]. The initial space-time distribution of the amplitude of the field entering the medium was made a Gaussian distribution. The statement of the

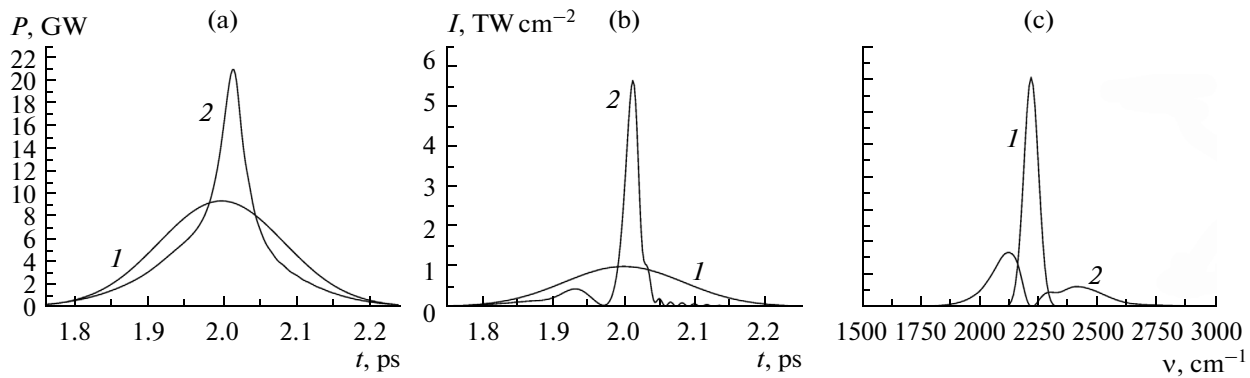


**Fig. 4.** Time profiles of (a) the radiation power and (b) on-axis intensity and (c) on-axis radiation spectrum at the input (curve 1) and the output ( $z = 1.25$  cm; curve 2).

problem specified the following parameters of the radiation pulse at the input:  $\lambda = 4.5$   $\mu\text{m}$ ,  $E = 2$  mJ, and half-amplitude duration  $t_{1/2} = 200$  fs. Figure 4 shows the results from calculations for input on-axis intensity  $I_0 = 1$   $\text{TW cm}^{-2}$ : the time profiles of the radiation power (Fig. 4a) and the on-axis intensity (Fig. 4b) at an input made from  $\text{CaF}_2$  with a thickness of 1.25 cm and at the output. Figure 4c shows the variation of the on-axis radiation spectrum.

When the input intensity was raised to  $1.5$   $\text{TW cm}^{-2}$ , the required  $\text{CaF}_2$  thickness dropped to 0.9 cm, and the duration of the on-axis output radiation fell from 19 ( $I_0 = 1$   $\text{TW cm}^{-2}$ ) to 16 fs; i.e., it was reduced to almost a single oscillation period. The calculated  $B$  integral value at the  $\text{CaF}_2$  outlet was as high as 6–8. The effect of small-scale self-focusing should be strong at such  $B$  integral values. To offset this effect, we must use intermediate spatial filters [4, 19]. The considered compressor is scalable: if the input radiation intensity is held constant and the compressor diameter is increased, the intensity and the duration of the output radiation remain the same, and only the output power increases. For example, the output pulse power is 2.4 TW for an input energy of 200 mJ and an on-axis input radiation intensity of 1  $\text{TW cm}^{-2}$ .

We thus found that the  $\text{CaF}_2$ -based compressor of femtosecond IR laser radiation with a wavelength of 4.5  $\mu\text{m}$  allows us to compress a 200-femtosecond pulse with an energy of 2 mJ (a power of 9.4 GW and an intensity of  $1.5$   $\text{TW cm}^{-2}$ ) to 16 fs (almost to a single period) on the axis and to 30 fs (two periods) in the near-axis region where up to 50% of the pulse energy is contained. The output power can be increased by a factor of 3–3.5. Note that the above design can be modified to increase the output energy and operate at a terawatt-level output power with an output energy of approximately 200 mJ. With the saturation energy being relatively low (about 30 mJ  $\text{cm}^{-2}$ ), the output energy depends to a considerable extent on the cross section and the length of the active element, and on whether high-energy pumping is available.

## CONCLUSIONS

A design for a subterawatt femtosecond laser system of the middle IR range was proposed. The system has the following output parameters: 4–5  $\mu\text{m}$ , 2 mJ, and 150–200 fs. The femtosecond seeder of mid-IR radiation was constructed on the basis of an optical parametric oscillator. The seeder parameters were 1–10  $\mu\text{J}$  and 200 fs. The  $\text{Fe}^{2+}:\text{ZnSe}$  laser was optically pumped using a specially constructed Q-switched YSGG:Cr:Er laser (with output energies as high as 100 mJ and pulse durations of 50 ns). The differential lasing efficiency with respect to the absorbed energy can be achieved for weak ultrashort (on the order of 100 fs) laser pulse. A circuit for the compression of femtosecond IR laser pulses in  $\text{CaF}_2$  by means of phase self-modulation based on the Kerr nonlinearity and anomalous group velocity dispersion was designed and analyzed. It was found that input pulses with durations of 150–200 fs can be compressed to 30 fs (approximately two optical cycles), while the initial power can be simultaneously increased by a factor of 3–3.5.

## ACKNOWLEDGMENTS

This work was supported by the Russian Science Foundation, project no. 14-12-00520.

## REFERENCES

1. Frolov, M.P., Korostelin, Yu.V., and Kozlovsky, V.I., *J. Russ. Laser Res.*, 2011, vol. 32, no. 6, p. 528.
2. Mirov, S.B., et al., *Opt. Mater. Express*, 2011, vol. 1, no. 5, p. 898.
3. Firsov, K.N., et al., *Laser Phys. Lett.*, 2014, vol. 11, p. 085001.
4. Bravy, B.G., Gordienko, V.M., and Platonenko, V.T., *Laser Phys. Lett.*, 2014, vol. 11, p. 065401.
5. Mirov, S., Fedorov, V., Moskalev, I., et al., *J. Lumin.*, 2013, vol. 133, p. 268.

6. Myoung, N., Martyshkin, D.V., and Fedorov, V.V., *Proc. SPIE*, 2011, vol. 7912, p. 79121C.
7. Gordienko, V.M., Grechin, S.S., Ivanov, A.A., et al., *Quantum Electron.*, 2006, vol. 36, no. 2, p. 114.
8. Gordienko, V.M., Djidjoev, M.S., Firsov, V.V., et al., *Proc. Int. Conf. on Laser Optics*, St. Petersburg, 2012.
9. Gordienko, V.M., Ivanov, A.A., Podshivalov, A.A., et al., *Laser Phys.*, 2006, vol. 16, no. 3, p. 427.
10. Moulton, P. and Slobodchikov, E., *Proc. CLEO:2011, Laser Science to Photonic Applications*, Baltimore, 2011.
11. Frantz, L. and Nodvik, J., *J. Appl. Phys.*, 1963, vol. 34, p. 2346.
12. Major, A., Aitchison, J., Smith, P., et al., *Proc. SPIE*, 2005, vol. 5971, p. 59710H.
13. Weber, M.J., *Handbook of Optical Materials*, New York: CRC Press, 2003.
14. Milam, D., Weber, M.J., and Glass, A.J., *Appl. Phys. Lett.*, 1977, vol. 31, p. 822.
15. Darginavicius, J., Majus, D., Jukna, V., et al., *Opt. Express*, 2013, vol. 21, no. 21, p. 25210.
16. Poole, R.T., Szajman, J., Leckey, R.C.G., et al., *Phys. Rev. B*, 1975, vol. 12, no. 12, p. 5872.
17. Couairon, A., Brambilla, E., Corti, T., et al., *Eur. Phys. J.: Spec. Top.*, 2011, vol. 199, p. 5.
18. Keldysh, L.V., *J. Exp. Theor. Phys.*, 1965, vol. 20, no. 5, p. 1307.
19. Voronin, A.A., Zheltikov, A.M., Ditmire, T., et al., *Opt. Commun.*, 2013, vol. 29, p. 299.

*Translated by D. Safin*